

1 HZ FLARING IN SAX J1808.4–3658: FLOW INSTABILITIES NEAR THE PROPELLER STAGE

ALESSANDRO PATRUNO¹, ANNA WATTS¹, MARC KLEIN WOLT¹, RUDY WIJNANDS¹, MICHIEL VAN DER KLIS¹

Draft version October 28, 2018

ABSTRACT

We present a simultaneous periodic and aperiodic timing study of the accreting millisecond X-ray pulsar SAX J1808.4–3658. We analyze five outbursts of the source and for the first time provide a full and systematic investigation of the enigmatic phenomenon of the 1 Hz flares observed during the final stages of some of the outbursts. We show that links between pulsations and 1 Hz flares might exist, and suggest they are related with hydrodynamic disk instabilities that are triggered close to the disk-magnetosphere boundary layer when the system is entering the propeller regime.

Subject headings: stars: individual (SAX J1808.4–3658) — stars: neutron — X-rays: stars

1. INTRODUCTION

The low mass X-ray binary transient SAX J1808.4–3658 (hereafter J1808) was discovered with *Beppo-SAX* in 1996 (in 't Zand et al. 1998) and was found to be an accreting millisecond X-ray pulsar (AMXP, Wijnands & van der Klis 1998) in 1998 when observed with the *Ross X-ray Timing Explorer (RXTE)*. Since then, four other outbursts have been observed with *RXTE*. The X-ray lightcurves of the 5 outbursts under consideration are remarkably similar in shape and duration. The typical outburst duration is several weeks with a recurrence time of ~ 2.5 yr; after 1998, outbursts occurred again in 2000, 2002, 2005 and 2008. The accretion rate increases steeply in the first 2–5 days of the outburst (*fast rise*), then it stays relatively high for a few days (*peak*), reaching at most a few percent of the Eddington rate. After this, the X-ray flux has a *slow decay* lasting ~ 10 days, before entering a *fast decay* stage in which the flux drops in 3–5 days. The source then enters a low flux state characterized by 3–5 day flares separated by intervals of very low luminosity, the *re-flaring* state that can last for months, followed by *quiescence*.

J1808 has shown 401 Hz pulsations during all the outbursts, at all the luminosities observable by *RXTE* ($\geq 10^{34}$ erg s⁻¹), even during the re-flares (Hartman et al. 2008, 2009a). The re-flaring state was observed to last ~ 60 days (MJD 53550 – 53610) in the 2005 outburst, followed by a low luminosity state approximately 10 times brighter than quiescence that lasted for another ~ 60 days (Campana et al. 2008). In the 1998 outburst the *RXTE* observations stopped immediately after the beginning of the re-flares, while in the 2000 outburst, only the re-flaring state was observed (for ~ 100 days, see Wijnands et al. 2001). Thanks to the good sensitivity of the *XMM-Newton* and *Swift-XRT* satellite, Wijnands (2003) and Campana et al. (2008) measured a minimum luminosity of $\sim 5 \times 10^{32}$ erg s⁻¹ between the flares in the re-flaring state in the 2000 and 2005 outburst (assuming a distance of 3.5 kpc). In 2002 (Wijnands 2004) and 2008 (Hartman et al. 2009a) the re-flaring state was observed with *RXTE* for approximately 1 month.

Campana et al. (2008) interpreted the observed low

luminosities as a signature of the onset of the propeller regime. The propeller regime is characterized by a Keplerian velocity in the innermost region of the accretion disk that is slower than the rotational velocity of the neutron star magnetosphere. In its original formulation (Illarionov & Sunyaev 1975) it was proposed to suppress the accretion flow onto the neutron star surface. The gas, carrying part of the neutron star angular momentum, was thought to be expelled and spin down the neutron star. Ghosh & Lamb (1979a,b) proposed that spin down and accretion could occur simultaneously and recent MHD simulations (Romanova et al. 2005, Ustyugova et al. 2006) show that two different propeller regimes are possible: a strong propeller, characterized by a strong outflow of gas, and a weak propeller, with no outflows. In both cases a magnetically channeled accretion flow onto the neutron star surface is still expected consistent with the 401 Hz pulsations observed.

Wijnands (2004) reported a modulation at a repetition frequency of ~ 1 Hz that completely dominates the lightcurve of J1808 in the 2000 and 2002 outbursts. This ~ 1 Hz modulation appears as sudden intensification of the X-ray flux that are obvious in the power spectra and sometimes are directly detected in the lightcurve. A re-analysis of these data, along with a complete investigation of this phenomenon for the other three outbursts (1998, 2005 and 2008), is presented in this paper.

The mechanism of the re-flares and the 1 Hz modulation is still unclear, but it might be related to the onset of instabilities expected for sources near the propeller stage (Ustyugova et al. 2006). It has been suggested that the fast decay and the re-flares are related to cooling and re-heating fronts propagating through the disk (Dubus, Hameury & Lasota 2001). The heating fronts change the accretion disk structure from a neutral to an ionized state, increasing the viscosity and the mass transfer rate through the inner accretion disk. If the inner disk structure is influenced by this process, the disk-magnetospheric boundary and/or the accretion process can be modified as well, possibly producing hydrodynamic instabilities in the accretion flow (Goodson, Winglee & Böhm 1997; Spruit & Taam 1993; Bildsten & Cutler 1995).

Whether the 1 Hz modulation is created by such instabilities is still an open question. J1808 provides a unique opportunity to study this, since it shows X-ray pulsations

arXiv:0904.0560v2 [astro-ph.HE] 11 Nov 2009

Electronic address: a.patruno@uva.nl

¹ Astronomical Institute “Anton Pannekoek,” University of Amsterdam, Kruislaan 403, 1098 SJ Amsterdam, Netherlands

that can be observed simultaneously with the aperiodic variability. One of the reasons why the pulsations can play an important role in understanding the mechanism behind the 1 Hz modulation is the pulse behavior observed during the 2002 outburst. A drift of ~ 0.2 cycles was observed in the pulse phases of the fundamental frequency (but not in the first overtone), starting and ending in coincidence with the beginning and the end of the fast decay (Burderi et al. 2006). The pulse phase starts to drift in coincidence with the beginning of the fast decay and ends when the re-flares appear. The interpretation of this drift is controversial.

Burderi et al. (2006) concluded that the phase drifts appear in coincidence with the onset of instabilities induced by accretion of matter onto a weakly magnetized star, such as motions of the hot spot on the neutron star surface. Hartman et al. (2008) concluded that the observed phase drift might have been due to a motion of the hot spot toward the magnetic pole as the inner accretion disk recedes with decreasing luminosity (and thus decreasing mass accretion rate).

In this paper, we present the first comprehensive analysis of the 1 Hz modulation and its relation to the re-flares and 401 Hz pulsations in all outbursts of J1808. We discuss possible explanations for the onset of the 1 Hz modulation and possible reasons why it has been observed only in J1808 until now. We suggest the onset of accretion flow instabilities when J1808 enters the propeller stage as the origin of the 1 Hz modulation.

2. X-RAY OBSERVATIONS AND DATA REDUCTION

2.1. *RXTE* observations

We reduced all the pointed observations with the *RXTE* satellite’s Proportional Counter Array (PCA, Jahoda et al. 2006) that cover the outbursts of J1808.

The aperiodic timing analysis was done using GoodXenon data with a time resolution of 2^{-20} s and Event data with a time resolution of 2^{-13} s. The data were binned into 1/8192 s bins including all 256 energy channels. We performed fast Fourier transforms (FFTs) of 128 s data segments, fixing the frequency resolution and the lowest available frequency to 1/128 Hz; the highest available Fourier frequency (Nyquist frequency) was 4096 Hz. No background subtraction or dead-time correction was made prior to the FFTs. The Poisson level was subtracted from the resulting power spectra. Following Klein-Wolt et al. (2004) we first estimated the Poisson noise using the Zhang et al. (1995) formula and then (after inspecting the high frequency range and finding no unexpected features) shifted it to match the level between ~ 3000 – 4000 Hz, where no intrinsic power should be present, but only counting statistics noise. Then we normalized the power spectra using the rms normalization (van der Klis 1995). In this normalization, the integral over the power spectrum is equal to the fractional rms amplitude squared. The power density units are $(\text{rms}/\text{mean})^2 \text{Hz}^{-1}$ and the fractional rms amplitude in one specific band is:

$$\text{rms} = \left[\int_{\nu_1}^{\nu_2} P(\nu) d\nu \right]^{1/2} \quad (1)$$

The errors on the fractional rms are calculated by using the dispersion of points in the data. We consider a

TABLE 1
RXTE AND *Swift*-XTE OBSERVATIONS ANALYZED FOR EACH OUTBURST

Outburst (year)	Start (MJD)	End (MJD)	Time (ks)	Program IDs
<i>RXTE</i>				
1998	50914.8	50939.6	160	30411
2000	51564.1	51604.6	130	40035
2002	52562.1	52604.8	664	70080
2005	53522.7	53587.9	267	91056,91048
2008	54731.9	54776.1	236	93027
<i>SWIFT</i>				
2008	54756.6	54778.3	15	0003003435-00030034044

measurement as a non-detection in a specific band, when the ratio between the fractional rms and its standard deviation is smaller than 3. In this case we quote upper limits at the 98% confidence level.

The periodic 401 Hz pulsations were analyzed by constructing pulse profiles folding chunks of lightcurve in profiles of $N = 32$ bins, with the ephemeris of J1808 provided by Hartman et al. (2009a). In this folding process we used the TEMPO pulsar timing program (v 11.005) to generate a series of polynomial expansions of the ephemeris that predict the barycentered phase of each photon detected. The length of each data chunk was chosen according to the length of each *RXTE* observation (Obs-Id).

We then split each pulse profile into a fundamental (at ν) and a first overtone (at 2ν) using standard χ^2 fits. For a detailed description of the method used for measuring the pulse time of arrivals (TOAs) we refer to Patruno et al. (2009). A set of pulse phase residuals was then obtained by subtracting a Keplerian circular orbit and constant pulse frequency model, using the ephemeris of Hartman et al. (2009a).

2.2. *Swift*-XRT observations

During the 2005 and 2008 outbursts, the *Swift* X-ray Telescope (*Swift*-XRT) observed the re-flaring state of J1808. We refer to Campana et al. (2008) for the study of the *Swift*-XRT 2005 observations. Here we consider 10 pointed observations (see Table 1) covering a total of ~ 15 ks that were taken during the 2008 outburst (MJD 54757–54778) and were reduced by using the XRT pipeline (v. 0.12.0). Each observation lasted between 1 and 3 ks. The data were collected in photon counting (PC) mode, except for observation 00030034041 which was taken in windowed timing (WT) mode.

We extracted source and background events for each observation using circular regions with radii of 20 arcseconds, and extracting photons with energies between 2–10 keV and 0.5–10 keV.

3. RESULTS

3.1. *The X-ray lightcurves and the re-flaring state*

In the 2008 outburst re-flaring state, the lightcurve reached very faint luminosities, with a large portion of the re-flares below the sensitivity limit of *RXTE*, but above the detection threshold of *Swift*-XRT. The flux reached a minimum level of $2.0 \times 10^{-13} \text{erg s}^{-1} \text{cm}^{-2}$ in the 0.5–10 keV band, which corresponds to a luminosity

of $\sim 3 \times 10^{32}$ erg s $^{-1}$ at 3.5 kpc. This luminosity is of the same order of magnitude as that observed by Wijnands (2003) and Campana et al. (2008) during the 2000 and 2005 re-flares.

A property of all the re-flares is the periodicity on time scales of a few days, creating the “bumps” observed in the lightcurve (see Fig. 1). The fast decay and the re-flares in the 2002 and 2005 show a similar duration. The 2008 outburst also shows comparable timescales, although with much higher uncertainty. As noted in § 1, in ’98 the observations stopped too early and the ’00 ones started too late to allow a similar comparison.

The precise determination of the re-flare periods suffers of biases due to occasional poor sampling and to the sensitivity limit of *RXTE*. Therefore, although the data certainly allow this, there is no significant evidence that differences in fast decay time scales between the 3 outbursts have an effect on the subsequent re-flare periodicity time scales.

In the 2008 outburst it is hard to calculate the re-flare time scale because the flux is below the sensitivity limit of *RXTE* in the majority of the observations. The *Swift* sampling was approximately 1 observation every 2 days, too long compared to the fast decay time scale of 3 days to unambiguously exclude shorter time scales. However, the fast decay and the re-flare time scales are again compatible with being the same.

In 2002 and 2005 the re-flares’ peak luminosity tends to decrease with time (see Fig. 1). This is not observed in the 2000 (see Wijnands et al. 2001) and 2008 re-flares, which show an erratic change of peak luminosities. In the re-flaring state, the luminosity can change by ~ 3 orders of magnitude on time scales of $\lesssim 1.5$ days (see Fig. 1 at MJD ~ 54756 and Wijnands 2003 for a similar observation in the 2000 outburst).

3.2. The fast decays and the pulse phase drifts

Close to the end of the 2002 outburst, the pulse phase of the fundamental was observed to drift by 0.2 cycles in just a few days, in coincidence with the beginning and the end of the fast decay (Burderi et al. 2006). Hartman et al. (2008) showed that a similar drift was present in 2005. Here we show that both phase drifts start and end in coincidence with (or very close to) the beginning and the end of the fast decay.

In Fig. 2 we plot the pulse timing residuals of the fundamental and the 2-10 keV X-ray flux in mCrab. In the 2002 outburst the pulse phase drift starts exactly when the fast decay begins. In the 2005 outburst we see the phase drift beginning close to the beginning of the decay, although given the large scatter in the pulse phases it is difficult to define the exact moment when the phases begin to drift. Both the 2002 and 2005 pulse phase drifts end in coincidence with the end of the fast decay. Both the 2002 and 2005 pulse phases drift by ~ 0.2 cycles.

The slope of the fast decay is consistent with being the same in both outbursts (see also Fig. 3). The pulse phases in both outbursts during this time drift at the same speed of ~ 0.07 cycle/day. The pulse phase behavior in the 2002 and 2005 fast decay is therefore consistent with being identical.

In the 2000 outburst a similar test cannot be performed since *RXTE* missed the decaying portion of the outburst, and the observations covered just the re-flaring state. In

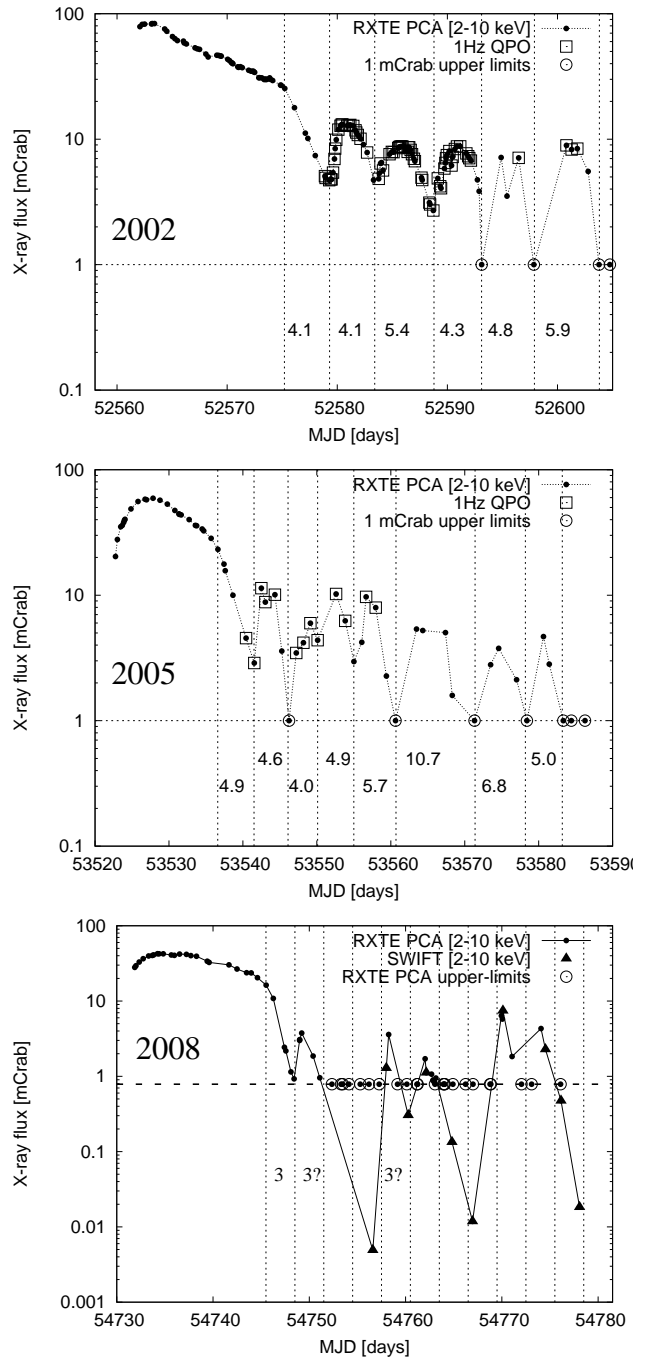


FIG. 1.— Outburst lightcurves in the 2-10 keV energy band. The count rate was normalized to the Crab intensity measurements nearest in time (Kuulkers et al. 1994) and in the same PCA epoch (e.g., van Straaten et al. 2003). Each black circle and triangle corresponds to one *RXTE* and *Swift*-XRT observation, respectively (see Table 1 for a complete list of the observations used). The open squares indicate observations when the 1 Hz QPO was detected, while the open circles indicate the *RXTE* observations with an X-ray flux below the detection threshold of ~ 1 mCrab. The vertical dashed lines divide the lightcurve into intervals beginning with the fast decay, and separating the re-flares. The duration of each re-flare is indicated in days and is similar to that of the fast decay (also indicated). In the 2008 outburst only few observations were above the detection threshold and all the vertical lines refer to the fast decay time scale.

the 1998 and 2008 outbursts no clear phase drift is observed. We refer to Hartman et al. (2008, 2009a) for

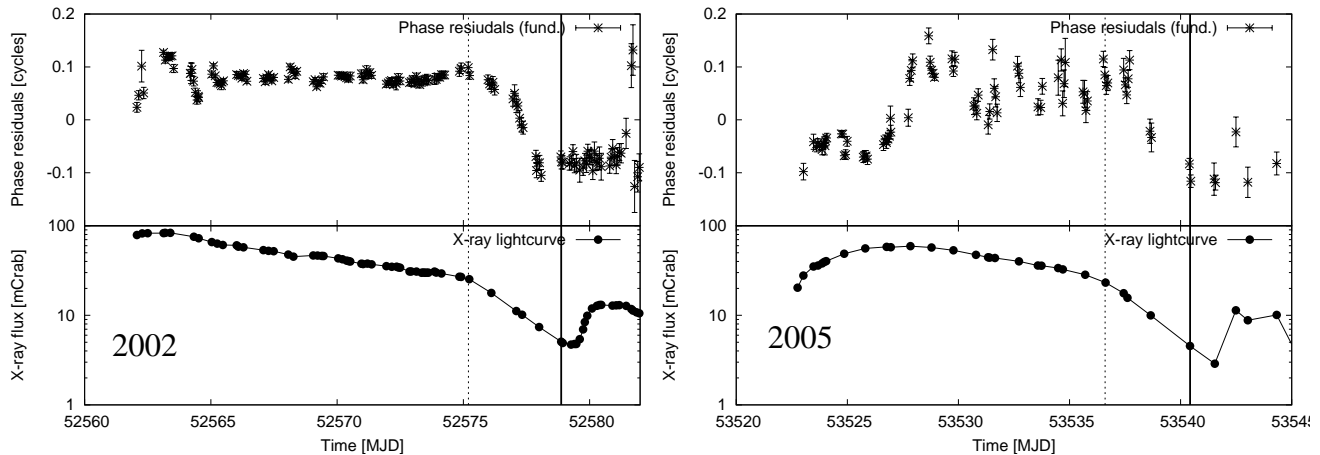


FIG. 2.— Pulse phase residuals (upper panels) calculated for the fundamental frequency alone. The bottom panels show the X-ray lightcurve (in logarithmic scale). The dashed lines mark the beginning of the fast decay in the lightcurves. At this point the pulse phases start to drift for ~ 0.2 spin cycles. The solid black lines mark the time of the first appearance of the 1 Hz QPO. Note that in both outbursts it appears at the end of the phase drift close to (but before) the minimum flux level in the X-ray lightcurve.

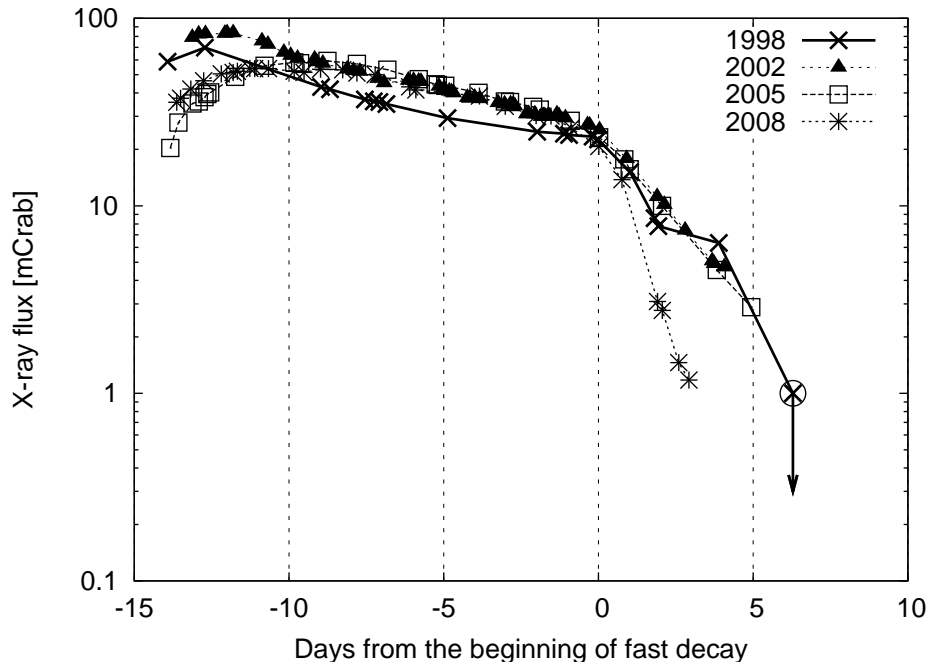


FIG. 3.— X-ray lightcurve of four outbursts, plotted up to the end of the fast decay stage. The curves are aligned to the beginning of the fast decay. The 2008 outburst has the shortest decay time. The 2008 slow decay, peak and fast rise stages are very similar to those of the 2005 outburst. The end of the 1998 outburst fast decay is limited by a non detection (open circle); it is the outburst that shows the dimmest luminosities before the beginning of the re-flares.

a detailed discussion of the coherent timing analysis of those two outbursts.

3.3. QPO parameters and flux

We will not in this paper provide a complete description of all the aperiodic variability observed in the 5 outbursts. For a description of the aperiodic timing features observed in AMXPs, we refer to van Straaten et al. (2005) and to the review of Wijnands (2006). Here we focus our attention on the 1 Hz modulation and give a brief description of the power spectra observed from the fast decay stage on, in order to provide context. A description of our quantitative analysis of the 1Hz modulation

follows in the next sections.

We examined the entire data set of all 5 outbursts for evidence of the 1 Hz modulation. Close to the end of the 2002 and 2005 pulse phase drifts, when the fast decay state is almost over, the X-ray lightcurve clearly shows this strong modulation with a repetition frequency of ~ 1 Hz (Fig. 4). It shows up as a strong quasi periodic oscillation (QPO) peak around 1 Hz in the power spectrum (Fig. 5, see also Wijnands 2004 for a similar plot for the 2002 outburst). Later during the re-flares of these outbursts the modulation occasionally recurs, as discussed in more detail in § 3.4. The 1 Hz modulation also appears and disappears sporadically during the re-flares of

the 2000 but was not detected in the 1998 and 2008 outbursts (cf. § 1).

We calculated the fractional rms amplitude² of the 1 Hz QPO by integrating the power in the 9.95 Hz wide band 0.05–10 Hz. This frequency band was chosen because it is here that the power is observed in the large majority of the observations. Some power above 10 Hz is observed in some cases as an extended tail of the 1 Hz QPO (Fig. 5), but selecting an upper frequency of 20 Hz does not change the results significantly. Clearly, using this method we sum up all the power from the different components in the power spectrum: power of the 1 Hz QPO, its harmonics, and the broad band noise. So everything in the range 0.05–10 Hz is included, and therefore this method is not optimal to measure the power generated by one single component. However, the rms calculated in this way is empirical and independent from any model used to fit the data. The fractional rms amplitude in the 0.05–10 Hz band was in the range 10–125% in all observations where the modulation was detected.

The QPO is usually quite broad, and its shape cannot be satisfactorily fitted by single or multiple Lorentzians, as it has a sharp fall-off in power at lower frequencies. In some observations a second harmonic peak is visible (Fig. 5). We model these features with Gaussians of the form:

$$P(\nu_i) = A \cdot \exp [(\nu_i - B)^2 / C^2] \quad (2)$$

where ν_i are the Fourier frequencies, A is a normalization factor, B is the centroid frequency (ν_0 or $2\nu_0$) and C is related to the FWHM through: $\text{FWHM} = 2C \cdot [\ln(2)]^{1/2}$. The typical value for the FWHM of the two Gaussians is ~ 1 Hz for all the three outbursts. The Gaussian that we use to fit the 1 Hz modulation usually has a quality factor $Q = \nu_0 / \text{FWHM} < 2$. When $Q < 1$ the power spectrum does not show a clear peak, but sometimes it does show a break in the noise (see for example the bottom panel in Fig. 5). Here we call the 1 Hz modulation “QPO” regardless of its quality factor. When $Q < 1$ we did not try to fit the power spectra with Gaussians because the centroid frequency is ill defined. When the 1 Hz QPO is fitted by 2 Gaussians ν_0 is defined as being the frequency of the Gaussian with the highest peak power in the power spectrum. With this choice ν_0 is consistent with being always the fundamental frequency of the 1 Hz modulation (varying between 0.8 and 1.6 Hz), as the harmonic peak at $2\nu_0$ is always lower in maximum power.

We calculated the fractional rms amplitude and centroid frequency of the 1 Hz QPO and the X-ray flux for the 2000, 2002 and 2005 outbursts. The fractional rms amplitude as observed in 2002 and 2005 is shown in Fig. 6 (middle panel). The fractional rms amplitude shows abrupt changes over time and does not follow a clear correlation with flux. In the 2000 re-flaring state, the 1 Hz modulation was detected in 13 observations out of 46, close to the peaks of the re-flares.

We plotted together all the points for the three outbursts in Fig. 7. There is a clear increase of the fre-

quency with flux and an anti-correlation between frequency and QPO fractional rms amplitude. Both relations have considerable scatter. We performed a rank correlation test on the 1 Hz QPO frequency vs. fractional rms anticorrelation and we found a Spearman coefficient of $\rho = -0.38$ with a probability of 0.1% of the null hypothesis (no correlation in the data) being true. A similar test for the frequency vs. flux correlation gives $\rho = 0.75$ with a probability of less than 0.01% for the null hypothesis.

We explored the fractional rms dependence of the 1 Hz QPO on the X-ray flux using a similar plot, and we found no clear dependence.

We then calculated the upper limits (quoted at the 98% confidence level) for all the observations after the end of the fast decay where the QPO was not detected. The upper limits were calculated per observation. In the 1998 data two complications occur: the observations ended immediately after the beginning of the re-flares, and the fast decay reached very faint fluxes (< 1 mCrab) at its minimum. Only in one observation J1808 was detected; then the upper limit was 55% rms. A 1 Hz modulation therefore cannot be completely excluded for this outburst. In 2000, 2002, 2005 and 2008 the most constraining upper limits are 15%, 9%, 19% and 19% rms, respectively.

Across the 2000, 2002 and 2005 outbursts, the 1 Hz QPO was observed in a rather narrow range of luminosities during the re-flares (2–15 mCrab, 2–10 keV), in contrast with the larger range of luminosities covered by the outbursts (~ 1 –80 mCrab). The *Swift*-XRT and *XMM*-Newton observations had insufficient time resolution or an insufficient number of counts to probe the presence of the 1 Hz QPO below 1 mCrab.

3.4. The appearance of the 1 Hz QPO

In the 2002 outburst, the 1 Hz QPO appears immediately after the pulse phase drift is complete, but with the flux still decreasing in the fast decay stage. In 2005 the 1 Hz QPO appears in a similar position (see black vertical lines in Fig. 2). In both the 2002 and 2005 outbursts, data gaps prevent the observation of the exact moment when the 1 Hz QPO appears. Taking account of the gaps, the flux level of the first 1 Hz QPO appearance is consistent between the two outbursts.

To track the appearance of the 1 Hz QPO on time scales as short as a few hundred seconds, we investigated the observation available in which the 1 Hz QPO first appears in the 2005 outburst. The observation (Obs-Id 91056-01-04-03) shows two chunks of data separated by a gap of 5000 s (chunk A with a length of 3200 s and chunk B with length 3500s) that we analyzed separately.

In chunk A the power spectrum has already changed with respect to the earlier observations: the power at higher frequencies has disappeared, and there is only power in the range 0.05–10 Hz. Probably we are witnessing the onset of the 1 Hz modulation. The average power spectrum shows a fractional amplitude of $(21 \pm 1)\%$ rms in the 0.05–10 Hz band. In chunk B we find a 1 Hz QPO clearly present with a fractional amplitude of $(68 \pm 4)\%$ rms.

We then calculated power spectra from 256 s data segments and determined the fractional rms amplitude in the 0.05–10 Hz band. (see Fig. 8). Significant power

² Fractional rms amplitude is standard deviation divided by mean flux. Values of rms larger than 100% indicate that the 1 Hz flares have a large amplitude and a short duty cycle. For a light curve composed exclusively of square flares with duty cycle f , $\text{rms} = \sqrt{\frac{1-f}{f}}$, arbitrarily large for $f \rightarrow 0$

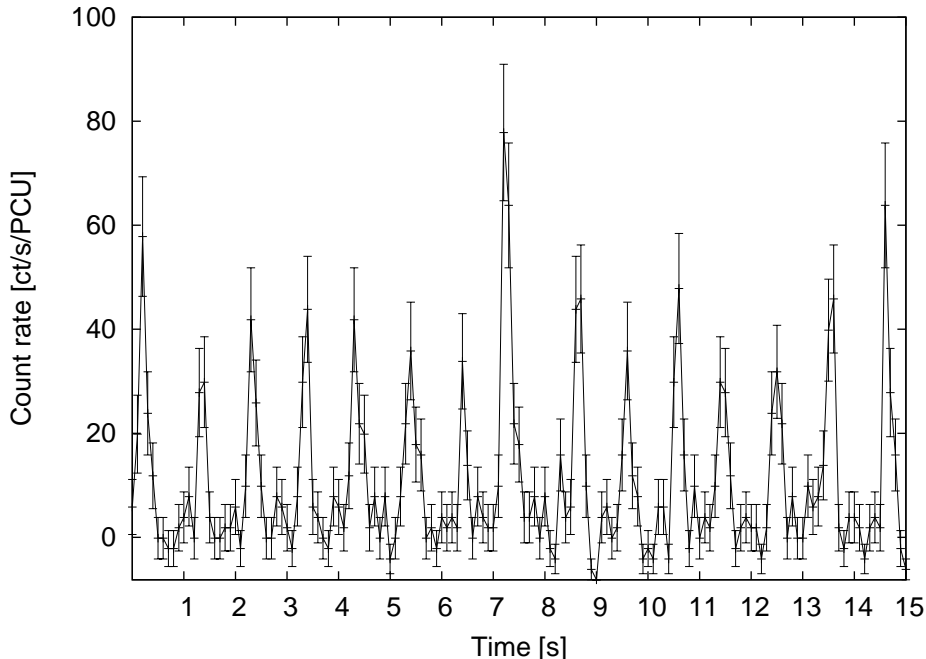


FIG. 4.— 1 Hz modulation of the X-ray lightcurve (background subtracted), as observed in a re-flare of the 2005 outburst. The figure shows a 15 s chunk of lightcurve with a time resolution of 0.1 seconds. In this observation the 1 Hz modulation has the highest measured fractional rms amplitude (125% rms, ObsId:91418-01-02-05).

is detected in three segments during the observations of chunk A, meaning that some low level activity is already present in the same frequency range where the QPO will later appear. In chunk B power is nearly always detected; the onset of the 1 Hz QPO must have occurred within the 5000 s gap. At MJD 53540.48 the amplitude shows an abrupt decrease from $\sim 60\%$ rms down to $< 30\%$ (98% confidence level) on a time scale of 256 s.

We also calculated the power in a number of frequency bands in the range 1/128 to 256 Hz for all power spectra of chunk A. The power is always consistent with zero at the three sigma level in all the frequency bands except for the 0.05-10 Hz band in the three segments mentioned above.

3.5. Energy dependence of the 1 Hz QPO

In Fig. 9 we show the energy dependence of the 1 Hz QPO. The points in the figure refer to the observation (one per outburst) for which the fractional rms of the 1 Hz QPO in the 2-60 keV energy band was the highest (110.5% rms in 2000, ObsId 40035-01-04-01, total exposure 7 ks; 117% rms in 2002, ObsId 70080-03-15-00, total exposure 2 ks; 125% rms in 2005, ObsId 91418-01-02-05, total exposure 1.2 ks). In these observations the characteristic frequencies of the 1 Hz QPO and its overtone form clear peaks in the power spectrum and $Q > 2$.

The energy spectrum is hard, rising by a factor of 1.5-1.7 between 2 and 17 keV. Upper limits (98 % confidence level) in the 17-60 keV band were: 114% rms for 2000, 157% rms for 2002 and 155% rms for 2005.

3.6. Jumps in 401 Hz pulse phases related to strength of 1 Hz QPO

During the first re-flare of the 2002 outburst, the 1 Hz QPO becomes very broad and then disappears. When

the QPO becomes very broad and its fractional rms amplitude suddenly drops from $\sim 50\%$ down to 10%, a jump of 0.2 cycles is observed in the pulse phases of the fundamental (**jump A**, see Fig. 6). Two similar pulse phase jumps of 0.1 cycles are observed (**jump B** and **C**) when the QPO is not detected, with rms amplitude upper limits of ~ 30 and $\sim 10\%$ rms (98% confidence level). We call these phase changes “jumps” as opposed to the “drifts” observed during the fast decay stage (§ 3.2), since the 0.1 – 0.2 cycle jumps are sudden, occurring on time scales of a few hours or less, while the 0.2 cycle drifts take 4 – 5 days.

In the 2005 outburst we see something very similar, although the re-flares have a sampling that is much worse: the observations are rather sparse and are separated by at least 1 day. In both the 2002 and 2005 outbursts, the pulse phase in the jumps is close to the pulse phase prior to the beginning of the fast decay stage (see § 3.2).

In the 2000 outburst the observations are rather sparse, with gaps of several days between observations. However also in this case when the QPO rms amplitude is low or the QPO is undetectable, the pulse phases are observed to jump by ~ 0.1 –0.2 cycles, consistent with the 2002 and 2005 pulse phase behavior.

This phenomenology relating the 1 Hz QPO rms amplitude and the pulse phases might suggest a link between the presence of the 1 Hz QPO and the accretion flow onto the neutron star surface. However, due to the sparse sampling of the observations and the small number of jumps observed, this link remains to be confirmed in future observations.

3.7. Dependence of 401 Hz pulsation on the 1 Hz phase

The 1 Hz modulation might affect the magnetic channeling during the re-flaring state. Possible differences in the pulse properties can be unveiled by analyzing the pul-

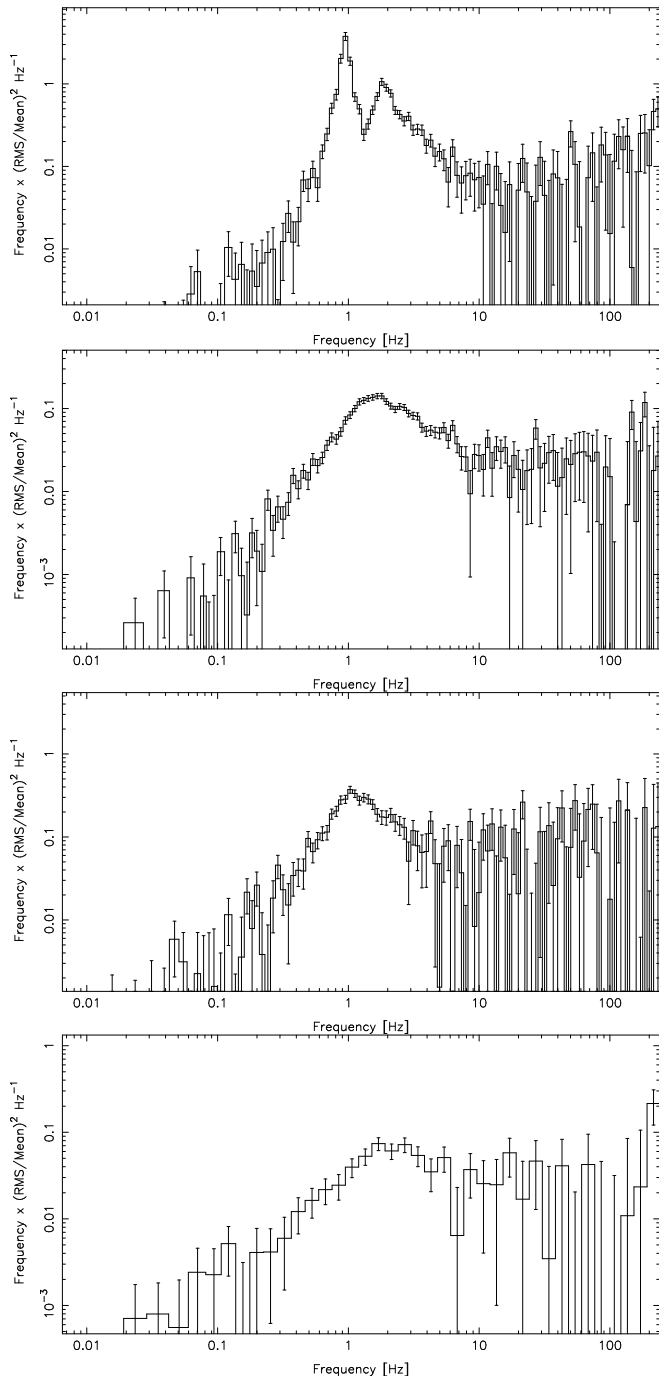


FIG. 5.— Power spectra (power \times frequency) of the re-flares of the 2005 outburst. The four plots show different manifestations of the 1 Hz modulation in the power spectrum. The upper panel (ObsId:91418-01-02-05, MJD \sim 53550.1) shows a strong coherent 1 Hz QPO and its overtone clearly separated. They blend together in the second panel (ObsId: 91418-01-01-00, MJD \sim 53542.5) where some power is also observed at frequencies higher than 10 Hz. The third panel (ObsId: 91056-01-04-01, MJD \sim 53541.5) shows a QPO with a steep cutoff at frequencies larger than \sim 10 Hz. The bottom panel (ObsId: 91418-01-03-04, MJD \sim 53556.7) shows still power, but as an incoherent feature without a clear peak.

sations coming from different phases of the 1 Hz modulation. Since the modulation has a frequency that changes with time, it is hard to unambiguously define its phase.

We therefore used a crude but simple approach, defining “peaks” and “valleys” of the 1 Hz modulation in the

lightcurve relative to the average flux. We first calculated the average X-ray flux per observation. Then we split the X-ray lightcurve into an upper half and a lower half containing peaks and valleys, respectively. We checked that this method was properly dividing the lightcurve by a visual inspection. We then folded all the peaks and the valleys into two different 401 Hz pulse profiles at the spin frequency of the neutron star (see Hartman et al. 2008 for the ephemeris used to fold the data), and repeated the procedure for each observation where the 1 Hz QPO was detected.

The pulse phases are always consistent with being the same for peaks and valleys, within the pulse phase uncertainty of down to 0.01 cycles. The absolute pulse amplitude is higher in the peaks than in the valleys but by a smaller fraction than the mean flux, so that the pulse fractional amplitude is *always* higher in the valleys by a factor varying between 1.2 and 6 (with a typical error on the amplitude ratios of \sim 0.1). The pulse amplitudes of peaks and valleys follow a similar evolution in time: when the pulse amplitude of peaks rises (or drops) in an observation, the same is seen for the pulse amplitude of valleys.

The valleys fractional rms amplitudes span a range between a few % rms up to more than 10 % rms, with values much larger than the average pulsed fractions of the persistent pulsation observed during the outbursts before the re-flares (for a discussion of the pulse fractional amplitudes during the 1998, 2000, 2002 and 2005 outbursts see Hartman et al. 2008 and for the 2008 outburst see Hartman et al. 2009a). The opposite is true for the pulsed fractions of peaks: they are on average smaller than the observed fractional amplitudes during the outbursts.

4. DISCUSSION

Our analysis of the five outbursts of SAX J1808.4-3658 has shown that the fast decay, the re-flares and the 1 Hz modulation can be related phenomena in the 2002 and 2005 outbursts (and possibly in the 2000 one) which might also affect the 401 Hz pulsations. The drifts in pulse phase and the re-flares observed on time scales of days might be related with some change in the disk structure which is connected to the fast decay, which takes place on a similar time scale. The fast decay presumably is either a thermal or a viscous one, and additionally depends on the lengthscale on which significant changes occur within the disk, longer length scales corresponding to longer time scales. The 1 Hz QPO properties had previously only been very briefly discussed in the literature, and left the mechanism responsible to be identified. We therefore studied the 1 Hz modulation properties in detail and related them to the behavior of the X-ray flux and the X-ray pulsations. Any suitable model for the 1 Hz modulation has to explain the following key properties that we reported in § 3:

- In 2002 and 2005, it appears at the end of the fast decay, after the pulse phases have drifted by 0.2 cycles (Fig 2)
- It appears at a flux level that is consistent in the 2002 and 2005 outbursts (§ 3.2)
- It appears sporadically only in a narrow range of luminosities (\lesssim 15mCrab, § 3.3).

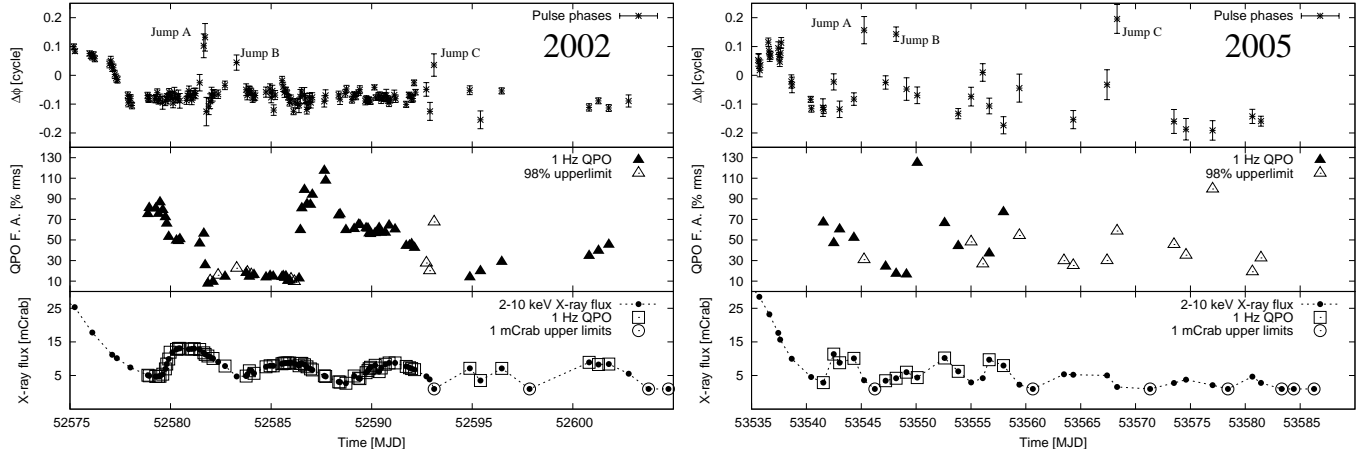


FIG. 6.— *Upper panels:* pulse phases of the fundamental for the 2002 and 2005 re-flaring states. *Central panels:* Fractional rms amplitude of the 1 Hz QPO (black triangles) and non-detections at 98% confidence level (open triangles). *Bottom panels:* 2-10 keV X-ray lightcurves. The observations where the 1 Hz QPO is significantly detected are marked with open squares, while measurements where the X-ray flux was below the sensitivity limit are marked with open circles. The pulse phase shows jumps of 0.1-0.2 cycles on a time scale of hours or less, when the 1 Hz QPO disappears or when its rms amplitude reaches a low level.

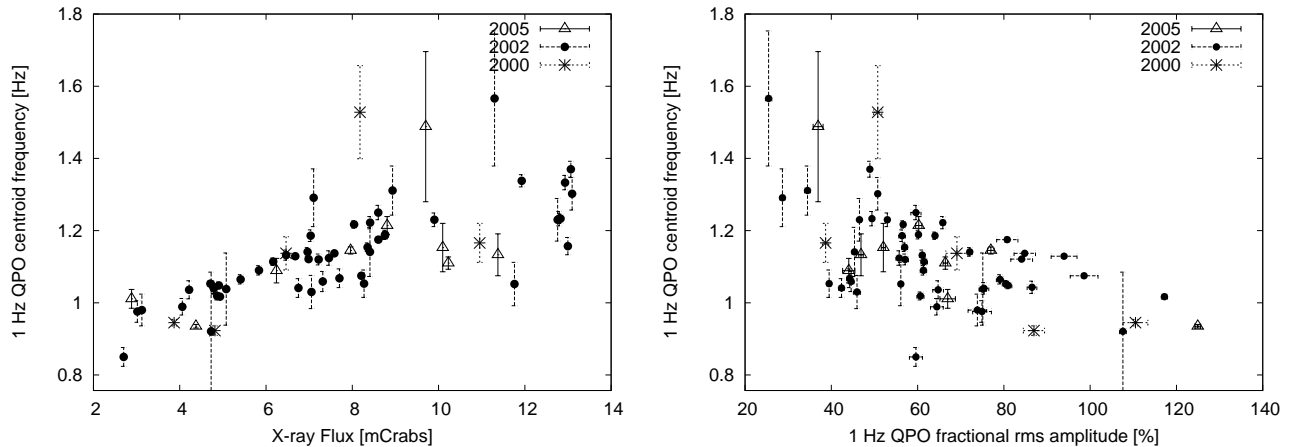


FIG. 7.— 1 Hz QPO centroid frequency vs. X-ray flux (left), 1 Hz QPO centroid frequency vs. 1 Hz QPO fractional rms amplitude (right panel) for the 2000 (asterisks), 2002 (circles) and 2005 (open triangles) outbursts. The QPO centroid frequency is clearly correlated with the X-ray flux and increases with decreasing fractional rms. The two relations are similar in all three outbursts.

- It is very coherent in some observations while in some others it is a broad incoherent feature (Fig. 4 and 5)
- In a few cases, its amplitude might be connected with the 401 Hz pulse phases (§ 3.6, Fig. 6).
- Its fractional rms amplitude can be as high as 125% and then 10% for the same X-ray luminosity (Fig. 6)
- Its amplitude is energy dependent, rising with energy up to ~ 17 keV (Fig. 9)
- Its rms amplitude is very high, up to 170% in the 10-16 keV band (Fig. 9)
- Its centroid frequency is quite stable and slightly increases with flux (Fig. 7)
- Its centroid frequency decreases with increasing fractional rms amplitude (Fig. 7)

Flares that might be similar to the J1808 re-flares are seen in other low mass X-ray binaries (LMXBs): the black hole candidate XTE J1650-500 (Tomsick et al. 2003), and the neutron star transient SAX J1750.8-2900 (Linares et al. 2008). This behavior therefore may not be unique to J1808, although this is the only AMXP in which such re-flares have been observed.

However, the 1 Hz modulation does appear to be nearly unique to J1808. The most similar QPOs, in terms of frequency and high fractional amplitude, are found in the systems that show Type II bursts. The Rapid Burster (Lewin et al. 1976; Hoffman, Marshall & Lewin 1978; Marshall et al. 1979) has QPOs in the range 0.04–4 Hz in the persistent emission, and from 2–5 Hz in during its Type II bursts (Tawara et al. 1982; Lewin 1987; Stella et al. 1988; Dotani et al. 1990; Lubin et al. 1991, 1992; Rutledge et al. 1995). Similar frequencies (0.04–0.4 Hz) have also been reported in the aftermath of Type II bursts from the bursting pulsar GRO J1744-28 (Komers et al. 1997). This similarity may point to a magne-

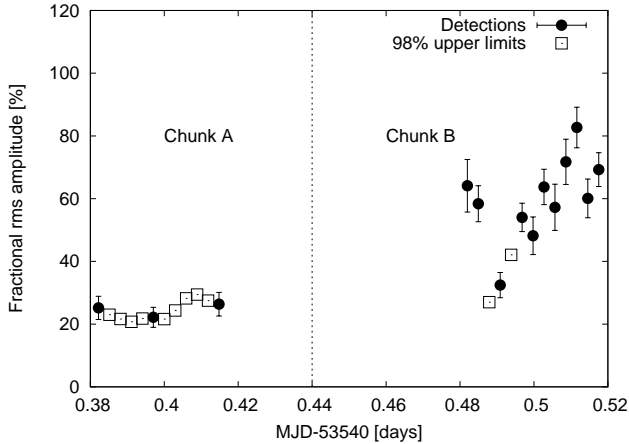


FIG. 8.— Temporal evolution of the 0.05-10 Hz fractional rms amplitude in observation 91056-01-04-03, showing the 1 Hz QPO appearance during the 2005 outburst. Each point corresponds to a 256 s long observation. Chunks A and B correspond to two different *RXTE* orbits. The black circles are $> 3\sigma$ detections, while the open squares are 98% confidence upper limits. The rms amplitude of chunk A is always below 30% rms, with 3 significant detections where the 1 Hz QPO is a broad incoherent feature in the 0.05-10 Hz band. In chunk B, the 1 Hz QPO fractional amplitude can reach values of up to $\sim 85\%$ rms and it fluctuates on very short time scales (~ 256 s).

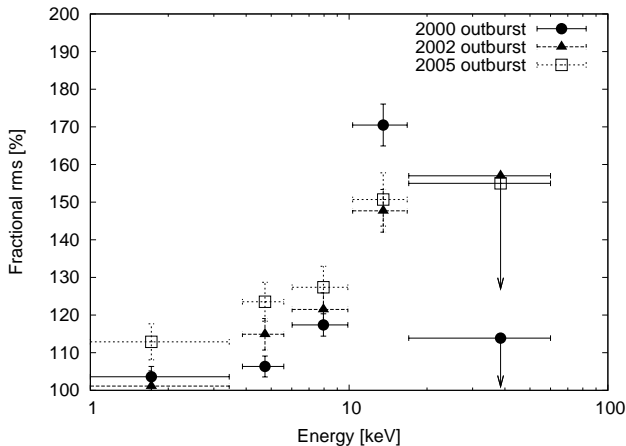


FIG. 9.— Energy dependence of the 1 Hz QPO fractional rms amplitude. The rms increases with energy for all the three outbursts. The plot shows rms amplitudes up to 17 keV, where a significant amount of counts is detected. In the range 17-60 keV only upper limits (98% confidence level) can be calculated for the three outbursts.

tosphere/disk mechanism (S 4.2).

Oscillations between 0.58 and 2.44 Hz were also reported in three dipping sources, although with an energy independent rms amplitude of below 12% (Homan et al. 1999; Jonker, van der Klis & Wijnands 1999; Jonker et al. 2000). Disk warping or shadowing was suggested as the most likely mechanism for these QPOs (see § 4.2.1).

Alternatively, the 1 Hz QPO may be caused either by the accretion flow (including possible occultation phenomena), or by some process that occurs after matter arrives on the surface. If the latter, it is very hard to understand why it is only seen in J1808. A brief consideration of the two most plausible surface mechanisms, global oscillations or marginally stable nuclear burning,

does in any case seem to rule them out.

There are various oscillatory modes of the neutron star surface layers that could lead to periodic brightness variations. The most likely candidates would be an ocean g-mode (a vibration driven by thermal buoyancy McDermott & Taam 1987; McDermott, van Horn & Hansen 1988), although to obtain a 1 Hz frequency would necessitate a very high order harmonic (Bildsten, Ushomirsky & Cutler 1996). The dependence of amplitude on energy could be explained by a mode model, but modes cannot explain the extremely high fractional amplitudes of the 1 Hz QPO (Piro & Bildsten 2006). In addition, if this was the right mechanism, then it should also be observed in other stars since the triggering conditions should not be unique to J1808.

The matter accreted onto the surface of the neutron star may burn stably, unstably (generating X-ray bursts), or in a marginally stable fashion (for a review see Bildsten 1998). The time scale for the quasi-periodic variations associated with marginally stable burning is set by the accretion time scale and the thermal time scale. For hydrogen ignition, the time scale for marginally stable nuclear burning, computed as in Heger, Cumming & Woosley (2007) using the appropriate accretion and thermal time scales, is clearly too slow (~ 10 minutes). For helium ignition, the time scales are shorter but still too slow (~ 100 s), thus ruling out the marginally stable nuclear burning scenario. In the following sections we therefore focus on the accretion flow as the most likely mechanism.

4.1. Accretion onto a magnetized neutron star

In order to understand what might be causing the 1 Hz QPOs, some general background on magnetically channeled accretion will be useful. To sustain channeled accretion at the maximum accretion rate of a few percent Eddington, the magnetic field for J1808 must be $\gtrsim 4 \times 10^7$ G (Hartman et al. 2008). The upper limit on the field, determined from timing, assuming that the spin down comes from magnetic dipole radiation from a rotation powered pulsar, is 1.5×10^8 G (Hartman et al. 2008, 2009a).

In a discussion of magnetized accretion, reference is often made to the corotation radius r_c , the radius at which matter in a Keplerian orbit would have the same angular velocity as the star.

$$r_c \sim 17 \left[\frac{\nu_s}{1 \text{ kHz}} \right]^{-2/3} \left[\frac{M}{1.4 M_\odot} \right]^{1/3} \text{ km} \quad (3)$$

where ν_s is the spin frequency of the neutron star and M is its mass. For J1808, assuming a mass of $1.4 M_\odot$, $r_c \sim 31$ km. The other radius of relevance is the magnetospheric radius r_m : the radius at which the magnetic field becomes dynamically important in controlling the inflow of matter. For spherically symmetric accretion, one can estimate r_m by setting the magnetic pressure equal to the ram pressure of free fall (Lamb, Pethick & Pines 1973):

$$r_m \sim 7.8 \left[\frac{B}{10^8 \text{ G}} \right]^{4/7} \left[\frac{R}{10 \text{ km}} \right]^{12/7} \left[\frac{M}{1.4 M_\odot} \right]^{-1/7} \times \left[\frac{\dot{M}}{\dot{M}_{\text{Edd}}} \right]^{-2/7} \text{ km} \quad (4)$$

where we have assumed a dipole field $B \sim \mu/r^3$, μ being the magnetic moment. R is the stellar radius and \dot{M} the accretion rate. In the case where accretion occurs from a disk this expression will be slightly modified by the rotational energy of the disk (Spruit & Taam 1993). Rotation of the central star can also affect the location of r_m (Lovellace, Romanova & Bisnovatyi-Kogan 1999).

This simple order of magnitude estimate yields 18 km for SAX J1808 at the peak of the outburst (assuming $\dot{M} = 5\% \dot{M}_{\text{Edd}}$ and $B = 10^8$ G). This increases as the accretion rate falls, becoming comparable to r_c once the accretion rate drops to 1% of the Eddington rate. The precise value of r_m will depend on details of inner disk physics as discussed in Psaltis & Chakrabarty (1999).

When $r_m < r_c$ accretion should proceed without difficulty, with the magnetic field channeling material out of the disk and onto the magnetic poles (Pringle & Rees 1972). Once $r_m > r_c$, however, the situation becomes more complex, and the system is said to be in the so-called ‘‘propeller’’ regime. Initially it was thought that for $r_m > r_c$ accretion would cease, with matter being expelled from the system (Illarionov & Sunyaev 1975). Further study by Spruit & Taam (1993) showed that r_m actually has to exceed r_c by a reasonable margin for material to be expelled. Steady accretion is in fact possible when $r_m > r_c$, even though the neutron star should spin down. In this stage the inner edge of the disk stabilizes near r_c and the density at the inner disk rises allowing angular momentum to be transferred outwards (Spruit & Taam 1993; Rappaport, Fregeau & Spruit 2004). This type of disk structure predicts spin-down without requiring penetration of the disk by the magnetic field far beyond r_c , as was proposed in early works on the topic (Ghosh & Lamb 1979b). In this paper we use the term ‘‘propeller’’ to define the condition in which $r_m > r_c$. In the next Section we will examine in turn the various mechanisms that might be responsible for the observed 1 Hz QPO.

4.2. Candidate Mechanisms: disk/magnetosphere instabilities

There are numerous ways of obtaining variability from the disk and its interactions with the stellar magnetosphere. Many have been explored, however, as a means of explaining the kHz QPOs - and so have frequencies that would be very far off 1 Hz. For this reason we will neglect many of the mechanisms for disk variability that have been discussed in the literature (see van der Klis 2006 for an extensive review of these mechanisms) and focus on those that might have frequencies in the right range.

4.2.1. Disk obscuration

The dipping QPOs have fractional amplitudes of $\sim 10\%$ (Homan et al. 1999; Jonker, van der Klis & Wijmands 1999; Jonker et al. 2000). In the dipping sources

the energy dependence of the QPO amplitude was flat, supporting the shadowing hypothesis. In J1808, there is a clear energy dependence and the 1 Hz QPO amplitude is much higher than that seen in the dippers. Furthermore, there is no evidence for dipping in the X-ray lightcurve of J1808. Several recent studies (Cackett et al. 2009, Papitto et al. 2009, Ibragimov & Poutanen 2009, Deloye et al. 2008) suggest an inclination for J1808 of around 60° which is too small to produce dipping. The mechanism proposed for this QPO was a partial obscuration of the neutron star surface via a blob of plasma in the disk, orbiting at a keplerian frequency of ~ 1 Hz. The disk radius corresponding to a keplerian frequency of 1 Hz is $r \sim 1700$ km. Considering the observer at an inclination of 60° , the blob of plasma needs to be as thick as 1000 km to allow partial obscuration of the neutron star surface. The expected accretion disk thickness at that radius is expected to be however orders of magnitude thinner than this value. By using for example Eq. (9) in Rappaport, Fregeau & Spruit (2004), the disk has an expected scale height of ~ 70 km. So, the 1 Hz QPO in J1808 is unlikely to be explained with a dipping mechanism.

Another possibility is the occurrence of occultations of the neutron star surface when the inner edge of the accretion disk enters in the line of sight of the observer. The 1 Hz QPO appears only at very low flux levels (in the range $\sim 0.001 - 0.01\%$ Eddington) which has two important consequences. First, by using Eq. 4, the inner edge of the disk is at approximately 56 km when the X-ray flux is at its minimum (0.001% Eddington). This means that, by assuming an observer inclination of 60° , the neutron star surface is obscured for a disk thickness of ~ 60 km. This thickness is however much larger than the expected disk scale height which is only 0.04 km. Moreover, even considering the physical size of the inner disk as large as 60 km, the optical depth would drastically reduce to values below 1 after a few km in height from the disk middle plane. Although the inner part of the accretion disk could be optically thin, allowing photoelectric absorption and thus explaining the hard energy dependence of the 1 Hz QPO rms amplitude, it cannot explain the very high rms amplitude of the QPO, since the optically thin plasma cannot completely obscure the neutron star surface.

4.2.2. Interchange instabilities

The role of interchange instabilities in admitting matter to the magnetosphere is discussed in detail by Arons & Lea (1976) and Elsner & Lamb (1977). The magnetic pressure prevents incoming matter from crossing magnetic field lines, but if it is energetically favorable (due for example to gravity) for material to be ‘‘inside’’ the field lines rather than ‘‘outside’’, then interchange instabilities can act to move the material inside. This is often referred to as the Rayleigh-Taylor instability, a term that refers to the instability that occurs when a more dense fluid overlies a less dense fluid in a gravitational field. Where a plasma is supported against gravity by a magnetic field, this is more correctly referred to as the Kruskal-Schwarzschild instability (Kruskal & Schwarzschild 1954).

The conditions necessary for the onset of Kruskal-Schwarzschild instabilities in the situation where $r_m \neq r_c$

have since been studied using MHD simulations (Romanova, Kulkarni & Lovelace 2008; Kulkarni & Romanova 2008). For misalignment angles $\theta \lesssim 30^\circ$ accretion can proceed either stably via funnel flows, or unstably via interchange instabilities. In the unstable situation matter accretes via a number of “tongues” that penetrate the magnetopause in the equatorial plane. If a certain number of tongues dominate, quasi-periodic oscillations can emerge in the light curves. Funnel flows can co-exist with accretion by tongues (Kulkarni & Romanova 2008), although their presence should reduce the amplitude of the persistent pulsations by reducing the azimuthal asymmetry (Romanova, Kulkarni & Lovelace 2008). This might be consistent with the continued presence of accretion-powered pulsations, with an amplitude that depends on the phase of the 1 Hz QPO.

In the cases studied by Romanova, Kulkarni & Lovelace (2008) interchange instabilities set in above a critical accretion rate, making them unlikely as a cause for the 1 Hz QPO (which appears only below a critical rate). Interchange instabilities cannot be completely ruled out, however. In the standard case studied by Romanova, Kulkarni & Lovelace (2008) magnetic pressure and gravity dominate the force equations. When $r_m \sim r_c$, however, magnetic pressure equals gravity. At this point other terms start to dominate the force equations and the character of the interchange instability will change (Baan 1977; Spruit & Taam 1993). Baan (1977) showed that sporadic penetration of the magnetosphere is possible in this regime. However detailed numerical simulations of the type performed at higher accretion rates have not been done, and the effect on funnel flows (and hence the amplitude of the accretion-powered pulsations) is not known. Without further study, periodicity due to interchange instabilities operating in the regime where $r_m \sim r_c$ cannot be ruled out as a mechanism for the 1 Hz QPO.

4.2.3. Magnetic reconnection instabilities

As matter moves within the disk (radially and azimuthally) it can drag magnetic field lines along with it. The sheared field lines can temporarily impede accretion until reconnection establishes a normal flow again. The resulting quasi-periodic accretion flow would lead to a corresponding quasi-periodicity in the lightcurve, provided that the accretion funnel and hot spot can respond on a 1 s time scale.

Magnetic reconnection is one of the most plausible mechanisms for Type II bursts (cf. § 4). Type II bursts are thought to occur in systems where magnetic inhibition causes accreting matter to build up in a reservoir outside the magnetosphere. Once a sufficient overdensity of material has accumulated, instabilities cause a catastrophic breach of the magnetospheric hammock, resulting in sudden bursts of accretion (Lewin et al. 1976). Dramatic changes in QPO properties immediately before Type II bursts, with no detectable change in the spectrum, have been interpreted as indicating that the QPOs in the persistent emission are generated within the fuel reservoir (Dotani et al. 1990). To what extent this phenomenon is relevant to our 1 Hz QPO is unclear. In the following discussion we explore several mechanisms that can produce 1 Hz oscillations.

Aly & Kuijpers (1990) used reconnection to explain

the QPOs observed in the Rapid Burster, and discussed how the disk would be broken up in ‘blobs’ by magnetic reconnection instabilities. They predict a frequency a few times the beat frequency between the rotation rate of the star ν_s and the Keplerian frequency at the inner edge of the disk ν_K . This implies that the frequency of the QPOs should pass through zero at the point where $r_m \sim r_c$.

An argument in favor of this mechanism is that has been observed in simulations (Goodson, Winglee & Böhm 1997; Goodson, Böhm & Winglee 1999; Goodson & Winglee 1999, and Romanova et al. 2005). Romanova et al. (2005) observed a strong quasi-periodicity associated with outflows of matter when the system was in the propeller regime. Unfortunately Romanova et al. (2005) do not model the emission mechanisms, so whether outflows or discrete accretion would genuinely lead to high amplitude QPOs in the X-ray emission is not clear. Ustyugova et al. (2006), using MHD simulations, showed that rapidly rotating accreting stars have strong periodicity of this type linked to strong outflows. Observationally, there is evidence for jet formation from the radio detections in the decay of the 1998 outburst and the peak of the 2002 outburst (Gaensler et al. 1999, Rupen et al. 2002), although the latter cannot be related with the propeller onset since it occurs at the maximum fluxes observed for J1808.

The frequency, for this mechanism, should depend on accretion rate (as observed, Fig. 7). It should however occur at all accretion rates: current models suggest no means of confining this mechanism to a narrow range of accretion rates as we observe for the 1 Hz modulation (§ 3.3). Another argument against this mechanism is that this type of instability should occur independently of field misalignment angle, so should be seen in all the AMXPs and the non-pulsating LMXBs (assuming that they all have an external magnetic field).

4.2.4. Thermal/viscous/radiation-driven instabilities

The inner region of an α disk (Shakura & Sunyaev 1973) is unstable to thermal and surface density perturbations (Pringle, Rees & Pacholczyk 1973; Lightman & Eardley 1974). Both types of instability can arise when radiation provides the major contribution to the total pressure (Shakura & Sunyaev 1976). Frank, King & Raine (2002) derive the various time scales in operation:

$$\tau_\phi \sim \tau_z \sim \alpha \tau_{\text{th}} \sim 10^{-4} \left[\frac{M}{1 M_\odot} \right]^{-1/2} \left[\frac{R}{10 \text{ km}} \right]^{3/2} s \quad (5)$$

$$\tau_{\text{visc}} \sim 3\alpha^{-4/5} \left[\frac{\dot{M}}{10^{16} \text{ g/s}} \right]^{-3/10} \left[\frac{M}{1 M_\odot} \right]^{1/4} \times \left[\frac{R}{10 \text{ km}} \right]^{5/4} s \quad (6)$$

The time scales are defined as follows: τ_ϕ is the dynamical time scale in the disk; τ_z is the time scale on which deviations from hydrostatic equilibrium in the z-direction get smoothed out; τ_{th} is the thermal time scale, that is the time scale for re-adjustment to thermal equilibrium, if, say, the dissipation rate is altered; and τ_{visc} is the

time scale on which matter diffuses through the disk due to the effect of viscous torques. Note that the canonical value suggested by numerical simulations for α is 0.01. Thus the dynamical time scale is of the order 10^{-4} s, the thermal time scale is 0.01 s and the viscous time scale is of the order 100 s assuming that the appropriate length scale is comparable to the inner disk radius $R \sim r_c \sim 10$ km. A study by King, Pringle & Livio (2007) shows that for many LMXBs $\alpha \sim 0.1$, an order of magnitude larger than the value suggested by numerical simulations of disks. Therefore the observed time scales are expected to be shorter than those calculated from numerical simulations. If the instability were confined to a narrow inner annulus of the disk, then this might be consistent with a 1 Hz frequency, since the viscous time scale falls for shorter lengthscales. In addition, if the instability triggers at the onset of the propeller regime when the inner edge of the disk puffs up to sustain accretion, this might explain the rarity of the phenomenon.

Instabilities which are known to operate at high accretion rates, such as thermal-viscous instabilities in radiation dominated disks (Taam & Lin 1984) and radiation-driven instabilities (Fortner, Lamb & Miller 1989; Miller & Park 1995), can be immediately ruled out since the 1 Hz QPO is observed at mass accretion rates of 0.001 – 0.01% Eddington.

An instability that might be relevant is the ionization instability that is thought to put the system into outburst in the first place (see Lasota 2001 for a detailed review). We know that the 1 Hz QPO appears at the end of the outburst, where current accretion disk models predict a transition from the hot to the cold state. The ionization instability might enter a marginally stable oscillatory state when the disk is on the verge of flipping between hot and cold regimes at luminosities of $\lesssim 1\%$ Eddington. The question is then why it would not occur always when the source is in the required luminosity range, and why not also in other transient LMXBs. Fine tuning by requiring this marginal state to coincide with for example the onset of the propeller regime and the associated changes in the disk structure as discussed above might resolve this. Therefore, the ionization instability, although unlikely, cannot be ruled out.

4.2.5. *Spruit-Taam instability*

The Spruit-Taam instability involves radial perturbations at the magnetospheric boundary (the inner edge of the accretion disk according to Spruit & Taam 1993). It relies on the viscosity in the disk to work, and does not require any shearing of the magnetic field. As discussed in Section 4.1, once $r_m \sim r_c$, accretion is only possible if the density at the inner edge of the disk rises. A small perturbation of the the disk radius away from $r_m = r_c$ will be immediately damped and the disk radius will return to the “equilibrium” position $r_m = r_c$ where inner disk edge and magnetosphere have the same angular velocity.

However, in the early propeller regime there exists a marginal state. When the inner accretion disk is at equilibrium, a given r_m corresponds to a specific density. If r_m moves inward a little bit, the boundary layer is ‘overdense’ compared to the equilibrium for that smaller r_m , and so quickly empties out. The rapid flow of matter from the inner edge of the disk causes the rest of the

co-rotating transition zone to empty out too. The rise in local \dot{m} pushes r_m in still further, reinforcing the perturbation. Eventually however the innermost layers are devoid of matter, since the viscous time scale further out in the disk is too slow to have replenished the inner regions. At this stage the boundary has to move back outward. Matter then accumulates again until the cycle restarts.

The time scale on which this instability operates is related to the viscous time scale just outside the corotating transition zone of the disk, since this sets the time scale for replenishment of the reservoir. However, this time scale is not related in a simple way to the viscous time scale as it also depends on parameters like the average accretion rate and the steepness of the transition between disk and magnetosphere.

According to eq.(6), the viscous time scale at r_c for J1808 is ~ 100 s, 2 orders of magnitude too long to explain the 1 Hz QPO. However this neglects the dependence of the time scale on the additional parameters and assumes that the appropriate length scale is comparable to the inner disk radius r_c . If a shorter length scale were involved then a shorter viscous time scale would be possible (Spruit & Taam 1993). To obtain a 1 second time scale, the length scale of the region of activity would need to be ~ 1 km, comparable to the scale of the inner “puffed up” regions in the steady state disk models calculated by Rappaport, Fregeau & Spruit (2004). The advantage of this mechanism is that the oscillatory state is expected to be active only in a very narrow range of radii from $r_m \simeq r_c$ to $r_m = 1.5r_c$ and hence a small range of accretion rates, as we observed for the 1 Hz QPO (see § 3.2).

The Spruit-Taam instability could modulate the accretion flow at high amplitude, which would fit the observations of very high fractional rms amplitudes for the QPO. The instability would also be compatible with the continued presence of accretion-powered pulsations, since accretion could still be funneled even if the inner edge of the disk were oscillating. Finally, the frequency of the instability has a weak dependence on the mass accretion rate (see Fig. 4 in Spruit & Taam 1993), rising or falling whether r_m is greater or less than r_c . This weak dependence has been observed in J1808 (Fig. 7) with the frequency rising with X-ray flux, thus suggesting $r_m > r_c$.

4.3. *The mechanism for the 1 Hz QPO*

In summary, most of the mechanisms examined cannot, based on our current understanding of how they work, explain key features of the 1 Hz QPO (see Table 2). The mechanisms that remain plausible are all associated with, or fine-tuned by, the onset of the propeller regime.

There are a number of other pieces of evidence (cf. § 1) that also point to major changes in the accretion environment at the luminosity where the 1 Hz QPO sets in (Wijnands et al. 2001, Wijnands 2003, Campana et al. 2008) - changes which might be explained by the onset of the propeller. In addition there are timing results suggesting a major change in disk structure around this time, such as the ~ 0.2 phase drift in the fundamental (arguing for a major change in the disk environment around this time), the change in the soft lag behavior (Hartman et al. 2009b), and the (debated) detection of an accretion torque (Burderi et al. 2006; Hartman et al.

TABLE 2
MECHANISMS FOR THE 1 Hz QPO

Model	Freq.	Amp.	Amp./Energy	Flux threshold	Freq./Flux.	Propeller
Surface oscillations	P	N	Y	N	...	N
Marginally stable nuclear burning	N	Y	...	N
Disk obscuration	Y	N	P	N
Interchange instability ($r_m \neq r_c$)	N	...	N
Interchange instability ($r_m \sim r_c$)	Y	...	Y
Magnetic reconnection instability	P	N	Y	N
Thermal/viscous instability	P	N	...	P
Ionization instability	P	Y	...	P
Radiation instability	N	N	...	N
Spruit-Taam instability	P	Y	...	Y	Y	Y

NOTE. — The table compares observed properties of the 1 Hz QPO to the various models discussed in §4. **Y/N** (yes/no) indicates that the model can/cannot explain the property in J1808 (e.g. at the accretion rates inferred for this source). The symbol **P** (possible) indicates that the model might be able to explain the property if certain conditions are met. An empty field indicates that the model makes no specific prediction for that property, and that further studies are required. Columns: (1) model, (2) 1 Hz QPO frequency, (3) high fractional amplitude, (4) energy dependence of the QPO fractional amplitude, (5) appearance of the oscillation below a certain flux threshold, (6) dependence of the centroid frequency on the X-ray flux. The last column shows whether the onset of the propeller regime is necessary for the model to be able to explain the observed QPO properties. Only models without **N** in any column remain viable, pending further study.

2008).

The mechanism proposed by Spruit & Taam (1993) seems to be the most promising candidate to explain the 1 Hz QPO, although the precise details of the time scales for this instability in the situation when funnel flows are relevant remain to be worked out. It has a precise onset point associated with the early propeller regime, should remain relatively stable in frequency as accretion rate varies slightly and is only expected in a narrow range of accretion rates.

Other mechanisms may also play a role, perhaps in concert with the Spruit-Taam instability. In § 4.2.2 we mentioned that new classes of interchange instabilities might operate near the propeller transition, perhaps leading to sporadic accretion. In § 4.2.4 we discussed the possibility of the ionization instability triggering on short length-scales in the inner regions of the disk once the source enters the propeller regime. This possibility is particularly plausible if the disk is already close to the transition from outburst to quiescence. The ionization instability might reinforce the Spruit-Taam instability mechanism, and could also fine-tune the onset conditions for the 1 Hz QPO (see § 4.4). The number of empty fields in Table 2 reflects the scale of the modeling work required to resolve these questions.

It is hard to understand why the 1 Hz QPO does not appear during the faint re-flares in the 2008 outburst. 8 out of 57 observations were in the 2–15 mCrab range during the re-flaring state. The reason why the 1 Hz QPO is not observed in these 8 observations is an open problem. Although poorly constrained, the 1998 outburst exhibited a similar behavior, and on several occasions during the 2000, 2002 and 2005 outbursts the 1 Hz QPO also remained undetected even for fluxes in the 2–15 mCrab range, with fractional rms amplitude upper limits of $\sim 10\%$. Clearly the 1 Hz QPO mechanism is not always triggered even in the 2–15 mCrab range in J1808.

In order to enter the propeller regime, J1808 needs to be at the point where $r_m \sim r_c$. Equating the crude expressions given in eq.(3) and (4), we obtain a relation between accretion rate, magnetic field and spin rate. Figure 10 shows the conditions for propeller onset for particular combination of these parameters. Clearly this is very approximate, since it is based on the simplest estimates of r_m and r_c , and ignores dependencies on mass and radius, but sufficient to understand whether the propeller scenario is a realistic possibility.

We plot the mass accretion rate values of three well known AMXPs: XTE J1807-294 (spin frequency 190 Hz), J1808 (401 Hz) and IGR J00291+294 (599 Hz). The first object was chosen because its spin frequency is one of the lowest known among AMXPs and its outburst spans a wide range of luminosities. IGR J00291+294 was chosen because its neutron star has the highest spin frequency known among AMXPs.

The mass accretion rates used in Fig. 10 are calculated for X-ray fluxes in the 2–10 keV energy band, by assuming a neutron star mass of $1.4 M_\odot$ and an efficiency of 10% for the conversion of rest mass energy of the accreted material into X-ray flux. Since these mass accretion rates do not refer to bolometric fluxes, they have to be considered lower limits. We also marked the bolometric *peak* luminosity of each source (as reported in Gierliński et al. 2002, Falanga et al. 2005a,b) for assumed distances of 8.5 kpc (IGR J00291+294³ and XTE J1807-294) and 3.5 kpc (J1808). The very broad range of luminosities of J1808 are observed thanks to the deeper observations of *Swift*-XRT (§ 3.1, Campana et al. 2008) and *XMM-Newton* (Wijnands 2003).

For all three sources, the conditions for propeller onset should be encountered if the field strength is $\sim 10^8$ G. For J1808, with a spin of 401 Hz and an accretion rate that runs from a few percent of Eddington at peak, down to less than 0.001 % in the dips between the re-flares, the system must always enter the propeller regime at

³ we note that IGR J00291+294 is not located toward the Galactic Center, therefore the assumed distance is arbitrary, and is made for an easier comparison with XTE J1807-294

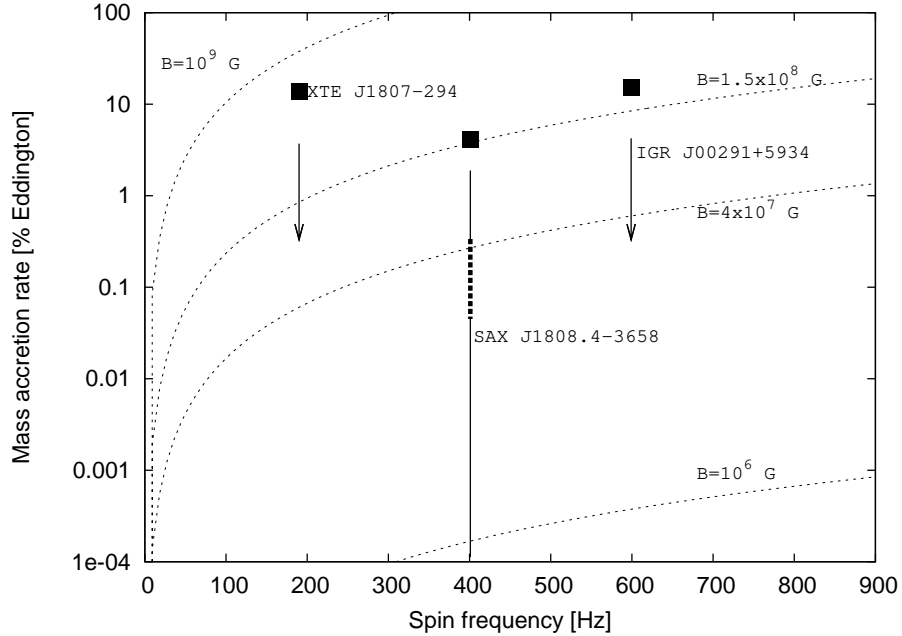


FIG. 10.— The accretion rate at which the propeller sets in for particular combinations of magnetic field and spin rate for the three AMXPs (dashed curves). The vertical arrows show the range of accretion rates over which the AMXPs have been observed and refer to *X-ray fluxes*. They have to be considered lower limits on the true mass accretion rates which are set by bolometric fluxes. The estimated *bolometric fluxes* at the peak of the outburst (where the mass accretion should be the highest) are marked with a black square (see text for details). The thick dashed vertical line in J1808 indicates the range of mass accretion rates at which the 1 Hz QPO has been observed.

same accretion rate, while for $B < 10^6$ G the system will not enter the propeller regime in the observed range of mass accretion rates. The range of magnetic fields is ($B \sim 0.4\text{--}1.5 \times 10^8$ G) as reported by Hartman et al. (2008, 2009a). The range of accretion rates for which the 1 Hz QPO appears (inferred from the 2-15 mCrab X-ray flux, § 3.2) lies just below this range. This coincidence is quite impressive since the accretion rates are lower limits.

By looking at Fig. 10 we can infer that the main reason why the 1 Hz QPO has been observed in J1808 and not in other AMXPs might be related with the proximity of J1808 (3.5 kpc) with respect to the other AMXPs (assuming they are all located at a distance close to 8.5 kpc). From a visual inspection of Fig. 10 the non-observation of the propeller in IGR J00291 could be problematic if the maximum accretion rate is $\sim 10\%$ Eddington and the magnetic field is $\sim 10^8$ G. However, many uncertainties can play a role here: uncertainties on the source distance, the conversion of X-ray luminosities into mass accretion rates, the precise condition for the onset of the propeller, not to mention all the uncertainties related with the definition of magnetospheric radius. In this sense Fig. 10 has to be taken as a qualitative picture, useful to understand the underlying behavior of this sources, but with too many uncertainties remaining to draw robust conclusions.

However, if we suppose that the instability is triggered in IGR J00291+5934 at the same mass accretion rates as in J1808, then the expected luminosity would be below the detection threshold of *RXTE*. None of the known AMXPs has been extensively monitored at low flux levels by *Swift*-XRT or *XMM-Newton*, both of which would be able to (easily) test this scenario.

If J1808 enters the strong propeller regime during the re-flares, a large outflow of gas is expected. Hartman et

al. (2008) and di Salvo et al. (2008) observed an anomalously large orbital period derivative. A possible explanation requires a mass loss from the system of $\sim 10^{-9} M_{\odot} \text{ yr}^{-1}$ (di Salvo et al. 2008 and Burderi et al. 2009 for a description of this scenario). The onset of a strong propeller with outflows of matter from the system can in principle play a role in this. If however, the real explanation is different (see Hartman et al. 2009a for a discussion of alternative possibilities to the strong outflow scenario) then the propeller might have only a minor role, if any, on the long term evolution of the orbital period.

A strong propeller might in principle explain the long term spin down of the neutron star in J1808 as proposed by Hartman et al. (2008). By assuming a B field of $\sim 10^8$ G, and assuming $r_m \sim 2r_c$ we can calculate the amount of mass that needs to be ejected in a strong propeller regime to produce the long term spin down observed by Hartman et al. (2009a) ($\dot{\nu} \sim -5.5 \times 10^{-16} \text{ Hz s}^{-1}$):

$$N_{sd} = N_{prop} \rightarrow 2\pi I \dot{\nu} = \sqrt{GM r_m} \dot{M}_{ej} \quad (7)$$

where N_{sd} is the spin-down torque, N_{prop} is the propeller torque (defined as in Bildsten 1998) and \dot{M}_{ej} is the amount of mass expelled during the strong propeller stage. The mass ejection required during quiescence is $\sim 8 \times 10^{-11} M_{\odot} \text{ yr}^{-1}$. This mass outflow is still insufficient to explain the large orbital period derivative observed in J1808. Moreover, even if the disk material is expelled at $r_m \sim 2r_c$, the viscous dissipation of gravitational potential energy would yield a luminosity of $\approx 10^{35} \text{ erg s}^{-1}$, which is too high when compared to the quiescence luminosity of J1808 ($\sim 5 \times 10^{31} \text{ erg s}^{-1}$, Campana et al. 2002, Heinke et al. 2009).

We have shown that the 1 Hz modulation has an effect on the 401 Hz pulse formation. Magnetic channeling is

expected to be easier in the valleys than in the peaks of the 1 Hz modulation, where the accretion rate is lower. We observed an increase of the 401 Hz pulsed fraction in the valleys in agreement with this. We have also found possible links between the 1 Hz modulation amplitude and the 401 Hz pulse phase. If the 1 Hz QPO reflects a change in the accretion flow, the position of the magnetic funnel can change accordingly, thus affecting the 401 Hz pulse phase. A better understanding of the process that generates the 1 Hz modulation would be fundamental to clarify this magnetosphere/disk interaction.

5. CONCLUSIONS

We have performed the first complete study of the 1 Hz modulation, its relation to the 401 Hz pulsations and the re-flares of SAX J1808.4-3658 as observed over 10 years. Several common features are observed in the 2000, 2002 and 2005 outbursts while the 1998 and 2008 outbursts have different properties, the most remarkable one being the absence of a strong 1 Hz modulation.

We focused on the origin of the 1 Hz oscillation that sometimes dominates the re-flare lightcurve and we found that all viable candidate mechanisms are connected with the onset of the propeller stage. The most promising model discussed is the Spruit-Taam instability which explains the stable 1 Hz frequency, its high amplitude and the narrow flux range of its occurrence in a natural way,

and is also compatible with the simultaneous presence of 401 Hz pulsations.

Many open issues remain. It is not clear yet why the pulse phase drifts by 0.2 cycles during the fast decay just before the onset of the 1 Hz modulation. It is also unclear whether the pulse phase jumps observed on time scales of hours or less are related with the amplitude of the 1 Hz. However, it is likely that this pulse behavior reflects changes in the accretion flow onto the surface triggered by flow changes associated with the 1 Hz QPO mechanism.

The reason why 1 Hz modulation has not been observed in other AMXPs might be the larger distance of the other sources making them undetectable in the relevant luminosity range. Future monitoring of low level flux states of other AMXPs will be very important to extend our comprehension of the 1 Hz modulation and further probe the onset of the propeller stage.

Acknowledgements: We would like to thank the *Swift* team for promptly scheduling the 2008 observations of SAX J1808.4-3658. We thank also P. Casella and D. Altamirano for useful discussions. We would also like to thank Henk Spruit for comments on an earlier version of this manuscript.

REFERENCES

- Aly J.J., Kuijpers J., 1990, *A&A*, 227, 473
 Arons J., Lea S.M., 1976, *ApJ*, 207, 914
 Baan W., 1977, *ApJ*, 214, 245
 Bildsten L., Cutler C., 1995, *ApJ*, 449, 800
 Bildsten L., Ushomirsky G., Cutler C., 1996, *ApJ*, 460, 827
 Bildsten L., 1998, in *The Many Faces of Neutron Stars*, eds Buccheri R., van Paradijs J., Alpar M.A., Dordrecht, Boston, Kluwer Academic Publishers, p.419
 Burderi L., Di Salvo T., Menna M.T., Riggio A., Papitto A., 2006, *ApJ*, 653, L133
 Burderi L., Riggio, A., di Salvo, T., Papitto, A., Menna, M. T., D’Ai, A., & Iaria, R. 2009, *A&A*, 496, L17
 Cackett, E. M., Altamirano, D., Patruno, A., Miller, J. M., Reynolds, M., Linares, M., & Wijnands, R. 2009, *ApJ*, 694, L21
 Campana, S., et al. 2002, *ApJ*, 575, L15
 Campana, S., Stella, L., & Kennea, J. A. 2008, *ApJ*, 684, L99
 Cannizzo J.K., 1997, *ApJ*, 482, 178
 Deloye, C. J., Heinke, C. O., Taam, R. E., & Jonker, P. G. 2008, *MNRAS*, 391, 1619
 di Salvo, T., Burderi, L., Riggio, A., Papitto, A., & Menna, M. T. 2008, *MNRAS*, 389, 1851
 Dotani T., Mitsuda K., Inoue H., Tanaka Y., Kawai N., Tawara Y., Makishima K., van Paradijs J., Penninx W., van der Klis M., Tan J., Lewin W.H.G., 1990, *ApJ*, 350, 395
 Dubus G., Hameury J.-M., Lasota J.-P., 2001, *A&A*, 373, 251
 Elsner R.F., Lamb F.K., 1977, *ApJ*, 215, 897
 Falanga, M., et al. 2005a, *A&A*, 436, 647
 Falanga, M., et al. 2005b, *A&A*, 444, 15
 Fortner B., Lamb F.K., Miller G.S., 1989, *Nature*, 342, 775
 Frank J., King A., Raine D., 2002, *Accretion power in astrophysics*, 3rd edition, Cambridge University Press
 Gaensler, B. M., Stappers, B. W., & Getts, T. J. 1999, *ApJ*, 522, L117
 Ghosh, P., & Lamb, F. K. 1979, *ApJ*, 234, 296
 Ghosh, P., & Lamb, F. K. 1979, *ApJ*, 232, 259
 Gierliński, M., Done, C., & Barret, D. 2002, *MNRAS*, 331, 141
 Goodson A.P., Winglee R.M., Böhm K.-H., 1997, *ApJ*, 489, 199
 Goodson A.P., Böhm K.-H., Winglee R.M., 1999, *ApJ*, 524, 142
 Goodson A.P., Winglee R.M., 1999, *ApJ*, 524, 159
 Hartman J.M., Patruno A., Chakrabarty D., Kaplan D.L., Markwardt C.B., Morgan E.H., Ray P.S., van der Klis M., Wijnands R., 2008, *ApJ*, 675, 1468
 Hartman, J. M., Patruno, A., Chakrabarty, D., Markwardt, C. B., Morgan, E. H., van der Klis, M., & Wijnands, R. 2009a, *ApJ*, 702, 1673
 Hartman, J. M., Watts, A. L., & Chakrabarty, D. 2009, *ApJ*, 697, 2102
 Heger A., Cumming A., Woosley S.E., 2007, *ApJ*, 665, 1311
 Heinke, C. O., Jonker, P. G., Wijnands, R., Deloye, C. J., & Taam, R. E. 2009, *ApJ*, 691, 1035
 Hoffman J.A., Marshall H.L., Lewin W.H.G., 1978, *Nature*, 271, 630
 Homan J., Jonker P.G., Wijnands R., van der Klis M., van Paradijs J., 1999, *ApJ*, 516, L91
 Ibragimov, A., & Poutanen, J. 2009, *MNRAS*, 392, 1322
 Illarionov A.F., Sunyaev R.A., 1975, *A&A*, 39, 185
 in ’t Zand, J. J. M., Heise, J., Muller, J. M., Bazzano, A., Cocchi, M., Natalucci, L., & Ubertini, P. 1998, *A&A*, 331, L25
 Jahoda, K., Markwardt, C. B., Radeva, Y., Rots, A. H., Stark, M. J., Swank, J. H., Strohmayer, T. E., & Zhang, W. 2006, *ApJS*, 163, 401
 Jonker P.G., van der Klis M., Wijnands R., 1999, *ApJ*, 511, L41
 Jonker P.G., van der Klis M., Homan J., Wijnands R., van Paradijs J., Méndez M., Kuulkers E., Ford E.C., 2000, *ApJ*, 531, 453
 King A.R., Pringle J.E., Livio M., 2007, *MNRAS*, 376, 1740
 Klein-Wolt, M., Homan, J., & van der Klis, M. 2004, *Nuclear Physics B Proceedings Supplements*, 132, 381
 Kommers J.M., Fox D.W., Lewin W.H.G., Rutledge R.E., van Paradijs J., Kouveliotou C., 1997, *ApJ*, 482, L53
 Kruskal M.D., Schwarzschild M., 1954, *Proc. R. Soc. London, Ser. A* 223, 348
 Kulkarni A.K., Romanova M.M., 2008, *MNRAS* in press, arXiv:0802.1759
 Kuulkers, E., van der Klis, M., Oosterbroek, T., Asai, K., Dotani, T., van Paradijs, J., & Lewin, W. H. G. 1994, *A&A*, 289, 795
 Lamb F.K., Pethick C.J., Pines D., 1973, *ApJ*, 184, 271
 Lasota, J.-P., 2001, *New Astronomy Reviews*, 45, 449
 Lewin W.H.G., Doty J., Clark G.W., Rappaport S.A., Bradt H.V.D., Doxsey R., Hearn D.R., Hoffman J.A., Jernigan J.G., Li F.K., Mayer W., McClintock J., Primini F., Richardson J., 1976, *ApJ*, 207, L95

- Lewin W.H.G., 1987, in *The origin and evolution of neutron stars*, Proceedings of the IAU Symposium, Nanjing, People's Republic of China, May 26-30, 1986 (A88-28476 10-90). Dordrecht, D. Reidel Publishing Co., p. 363-374.
- Lightman A.P., Eardley D.M., 1974, ApJ, 187, L1
- Linares, M., Degenaar, N., Wijnands, R., & Altamirano, D. 2008, *The Astronomer's Telegram*, 1777, 1
- Romanova, M. M., Kulkarni & Lovelace, R. V. E. 2005, ApJ, 635, L165
- Lovelace R.V.E., Romanova M.M., Bisnovatyi-Kogan G.S., 1999, ApJ, 514, 368
- Lubin L.M., Lewin W.H.G., Tan J., Stella L., van Paradijs J., van der Klis M., Penninx W., 1991, MNRAS, 249, 300
- Lubin L.M., Lewin W.H.G., Rutledge R.E., van Paradijs J., van der Klis M., Stella L., 1992, MNRAS, 258, 759
- Marshall H.L., Hoffman J.A., Doty J., Lewin W.H.G., Ulmer M.P., 1979, ApJ, 227, 555
- McDermott P.N., Taam R.E., 1987, ApJ, 318, 278
- McDermott P.N., van Horn H.M., Hansen C.J., 1988, ApJ, 325, 725
- Miller G.S., Park M.-G., 1995, ApJ, 440, 771
- Papitto, A., Di Salvo, T., D'Ai, A., Iaria, R., Burderi, L., Riggio, A., Menna, M. T., & Robba, N. R. 2009, A&A, 493, L39
- Patruno A., Hartman J.M., Wijnands R., Chakrabarty D., van der Klis M., 2009, submitted to ApJ
- Piro A.L., Bildsten L., 2006, ApJ, 638, 968
- Pringle J.E., Rees M.J., 1972, A&A, 21, 1
- Pringle J.E., Rees M.J., Pacholczyk A.G., 1973, A&A, 29, 179
- Psaltis D., Chakrabarty D., 1999, ApJ, 521, 332
- Rappaport S.A., Fregeau J.M., Spruit H., 2004, ApJ, 606, 436
- Romanova, M. M., Ustyugova, G. V., Koldoba, A. V., & Lovelace, R. V. E. 2005, ApJ, 635, L165
- Rupen, M. P., Dhawan, V., Mioduszewski, A. J., Stappers, B. W., & Gaensler, B. M. 2002, IAU Circ., 7997, 2
- Rutledge, R. E., Lubin, L. M., Lewin, W. H. G., Vaughan, B., van Paradijs, J., & van der Klis, M. 1995, MNRAS, 277, 523
- Shakura, N. I., & Sunyaev, R. A. 1973, A&A, 24, 337
- Shakura N.I., Sunyaev R.A., 1976, MNRAS, 175, 613
- Spruit H.C., Taam R.E., 1993, ApJ, 402, 593
- Stella L., Haberl F., Lewin W.H.G., Parmar A.N., van Paradijs J., White N.E., 1988, ApJ, 324, 379
- Taam R.E., Lin D.N.C., 1984, ApJ, 287, 761
- Tawara Y., Hayakawa S., Hunieda H., Makino F., Nagase F., 1982, Nature, 299, 38
- Tomsick, J. A., Kalemci, E., Corbel, S., & Kaaret, P. 2003, ApJ, 592, 1100
- Ustyugova G.V., Koldoba A.V., Romanova M.M., Lovelace R.V.E., 2006, ApJ, 646, 304
- van der Klis, M. 1995, *The Lives of the Neutron Stars*, 301
- van der Klis M., 2006, *Rapid X-ray Variability*, in Compact stellar X-ray sources, eds Lewin W., van der Klis M., Cambridge Astrophysics Series, No. 39, Cambridge, UK: Cambridge University Press, pp.39-112
- van Straaten, S., van der Klis, M., & Méndez, M. 2003, ApJ, 596, 1155
- van Straaten, S., van der Klis, M., & Wijnands, R. 2005, ApJ, 619, 455
- Wijnands R., Méndez M., Markwardt C., van der Klis M., Chakrabarty D., Morgan E., 2001, ApJ, 560, 892
- Wijnands, R., & van der Klis, M. 1998, Nature, 394, 344
- Wijnands, R. 2003, ApJ, 588, 425
- Wijnands, R. 2004, Nuclear Physics B Proceedings Supplements, 132, 496
- Wijnands, R. 2006, Trends in Pulsar Research, 53
- Zhang, W., Jahoda, K., Swank, J. H., Morgan, E. H., & Giles, A. B. 1995, ApJ, 449, 930